Mecánica Computacional Vol. XXI, pp. 2213–2226
S. R. Idelsohn, V. E. Sonzogni and A. Cardona (Eds.)
Santa Fe–Paraná, Argentina, October 2002

AERODYNAMIC INSTABILITY OF SLENDER STRUCTURES SUBJECTED TO WIND ACTION

Jorge D. Riera[†]**, Daniel Ambrosini**[*]**,**
Letícia F. F. Miguel[†]**, Tatiana T. Oliveira**[†]**, João Kaminski Jr.**[†]

[*] Instituto de Estructuras
Universidad Nacional de Tucumán, CONICET
Avenida Independencia, 1800. Tucumán, Argentina
e-mail: dambrosini@herrera.unt.edu.ar, web page: http://www.unt.edu.ar

[†] Programa de Pós-Graduação em Engenharia Civil (PPGEC)
Universidade Federal do Rio Grande do Sul (UFRGS)
Avenida Osvaldo Aranha, 99 / 3º andar. 90035-190. Porto Alegre, RS, Brasil
e-mail: riera@ppgec.ufrgs.br, web page: http://www.ppgec.ufrgs.br

Key words: Structural Instability, State Variables, Frequency Domain, Fluid-Structure Interaction.

Abstract. *Atmospheric wind close to the ground surface may usually be modelled as a Gaussian stationary random process. The expected value and the power spectral density function are used to characterize this process. In previous works, has been developed a scheme of structural analysis that incorporates the wind action for a Monte Carlo simulation procedure of a Gaussian stationary random process, correlated in vertical sense. A numerical integration method is used in the frequency domain. As structure model a general formulation of beams is adopted with constitutive law general linear viscoelastic. Besides, the fast Fourier transform (FFT) algorithm is used to work in the frequency domain. The focus is particularly appropriate for the determination of the dynamic response of towers and chimneys to the longitudinal wind action, having been employed with excellent results to obtain the response of structures excited by the atmospheric turbulence, for which experimental evidence exists in the specialized literature. In this paper the model is extended for the determination of field matrix in the state space formulation, considering the linearized equations of motion for the effect of fluid-structure interaction.*

1. INTRODUCTION

Fluid flow around a flexible structure may cause changes in its basic dynamic properties, such as natural frequencies or damping. On the other hand, the dynamic pressures due to the fluid flow are altered by the motion of the structure. Therefore there is a flow of energy from the fluid toward the structure and vice versa, in a process commonly known as *aeroelastic effect* or *fluid-structure interaction*. The response of the structure under these conditions can be significantly different from that foreseeable from its initial properties.

This phenomenon has wide implications in engineering, from the design of intermediate and long span bridges, to pipe bundles in heat exchangers or vibrations of iced conductors, not to mention some of the most important problems of Aeronautical Engineering. In spite of the importance of this problem, there is yet no comprehensive theory or global model available. The so-called pseudo-static theory, as presented and used by Brito and Riera[1,2,3], is a global approach to the problem, at least for two-dimensional situations. In those contributions, the authors suggested a general procedure to obtain the interaction forces, which depend primarily on displacements and velocities of the body, for a cylindrical or prismatic body subjected to non-uniform flow. The resulting equations are applicable to many well-known problems in Wind Engineering, from simple galloping to more complex problems of flutter.

The aeroelastic effect has been subject of numerous studies, especially after the collapse of the first Tacoma Narrows Bridge in 1940. In this context, the state of the art analysis of bridges subjected to wind loading presented by Hudson *et al*[4] and Scanlan and Jones[5], as well as the most recent contributions of Cooper *et al*[6], Larsen[7] and Chen *et al*[8] may be mentioned.

With the purpose of analysing line-like structures under random dynamic loading, Ambrosini *et al*[9] developed a scheme that accounts for turbulent wind action using Monte Carlo simulation for a two-dimensional Gaussian stationary random excitation process, correlated in the vertical direction. Numerical integration is used in the frequency domain to solve the equations of motion in state space. The structural model is based on a general formulation for open section, thin-walled beams of a general linear viscoelastic material. The method is particularly appropriate for the determination of the dynamic response of structures to along- and accross-wind action.

In this paper the model is extended to the determination of the linearized field matrix in the state space formulation, considering the effect of fluid-structure interaction as previously proposed by Brito and Riera[1,2,3].

2. MODEL OF THE STRUCTURE

The model of the structure, schematically shown in Fig.1, is based on Vlasov's theory of thin-walled, open-section beams. The theory was modified to include the effects of shear flexibility, variable cross-sectional properties and rotatory inertia by Ambrosini *et al*[10.11], who derived the equations of motion in the state space, as described in the following.

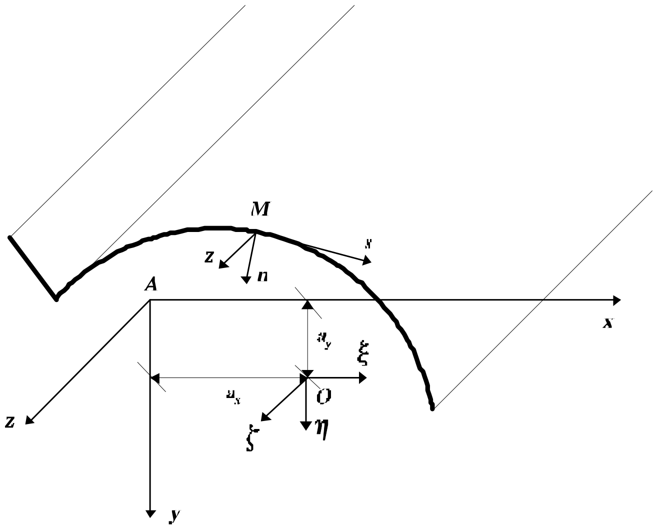

Figure 1: Model of the structure

The constitutive law for a general linear viscoelastic material is adopted, which allows the consideration of arbitrary linear damping in the structure. After transforming the equilibrium equations and the expressions that relate the bending and torsional moments, as well as the shear stress resultants, with the displacement variables into the frequency domain, a system in state variables with twelve coupled first-order differential equations is obtained. Adopting as state variables the displacements according to the x and y axes, ξ and η, the bending rotations with respect to those axes, ϕ_x and ϕ_y; the normal shear stress resultants Q_x and Q_y; the bending moments M_x and M_y; the rotation of the cross-section around its shear centre and its spatial derivative θ and θ', the total torsional moment M_T and the bimoment B; the state vector $\vec{v}$ is:

$$\vec{v}(z,\omega)=\{\eta,\ \ \phi_y,\ \ Q_y,\ \ M_x,\ \ \xi,\ \ \phi_x,\ \ Q_x,\ \ M_y,\ \ \theta,\ \ \theta',\ \ M_T,\ \ B\}^T \qquad (1)$$

The resulting system may be written in the form:

$$\frac{\partial \vec{v}}{\partial z}=\boldsymbol{A}\vec{v}+\vec{q} \qquad (2)$$

In which $\boldsymbol{A}$ denotes the system matrix and $\vec{q}$ the external load vector:

$$\vec{q}(z,\omega)=\{0,\ \ 0,\ \ -q_y,\ \ 0,\ \ 0,\ \ 0,\ \ -q_x,\ \ 0,\ \ 0,\ \ 0,\ \ -m_A,\ \ 0\}^T \tag{3}$$

q_x and q_y are externally applied loads per unit length and m_A is the external torsional moment per unit length. Note that, for simplicity, the same notation will be used for the state variables as well as for their transforms, since the domain can be adequately identified by indication of the function arguments. For example, $\eta(z,t)$ and $\eta(z,\omega)$ denote the y-displacement in the time domain and to its Fourier transform, respectively.

In the following, the equations of motion, as well as all functions, including the viscoelastic constitutive law, are divided in its real and imaginary parts. The system consists thus of 24 equations and 24 unknowns. The final matrix is presented in Appendix A.

Obviously, in numerical applications a fast Fourier transform algorithm (FFT) must be employed. Thus, for each frequency ω, the problem defined by equations (2) must be solved using standards numerical integration methods, jointly with techniques for transforming the boundary value problem in an initial value problem (Pestel and Leckie[12]). If this procedure is repeated for all frequencies ω in the range of interest, the FFT of all components of the state vector can be obtained. Finally, the solution in the time domain of all variables of interest can be determined by calculateting the inverse FFT of the corresponding variables in the frequency domain.

3. CONSIDERATION OF FLUID-STRUCTURE INTERACTION

Brito and Riera[1,2,3] developed linearized equations to represent the aerodynamic forces acting on flexible bodies, taking into consideration the motion of the body as well as the characteristics of the flow. According to the so-called *quasi-static theory:*

$$F_x=\frac{1}{2}\rho V_r^2 bC_x(\alpha,\dot{\theta}) \tag{4a}$$

$$F_y=\frac{1}{2}\rho V_r^2 bC_y(\alpha,\dot{\theta}) \tag{4b}$$

$$M=\frac{1}{2}\rho V_r^2 b^2 C_M(x,\dot{\theta}) \tag{4c}$$

In which F_x and F_y denote the forces exerted by the fluid, per unit length of body, in the x e y directions, respectively; M is the torsional moment around the body axis, V_r the incident wind velocity, as shown in Fig. 2. Additionally, ρ is the specific mass of the fluid, b is a characteristic cross-sectional dimension, usually a body dimension normal to the flow, while C_x, C_y and C_M are non-dimensional aerodynamic coefficients that depend on the shape of the cross-section, the angle of incidence α and the angular velocity of the body (shown in Fig. 2). Developing equations (4) as power series and neglecting higher-order terms, the following set of equations may be obtained (Brito and Riera[1]):

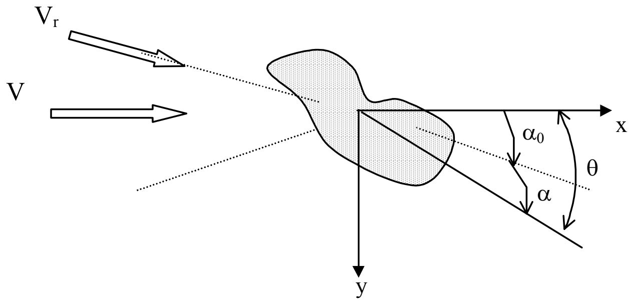

Figure 2: Definition of incident velocity vector

$$\vec{p} = \begin{Bmatrix} F_x \\ F_y \\ M \end{Bmatrix} = \frac{1}{2}\rho b V_0^2 \begin{Bmatrix} C_D \\ C_L \\ C_T \end{Bmatrix} + \frac{1}{2}\rho b V_0^2 \mathbf{A} \begin{Bmatrix} u \\ v \\ \theta \end{Bmatrix} + \frac{1}{2}\rho b V_0^2 \mathbf{B} \begin{Bmatrix} \dot{u} \\ \dot{v} \\ \dot{\theta} \end{Bmatrix} \tag{5}$$

in which V_0 is the wind velocity in the free field, C_D is the drag coefficient in the wind direction, C_L is the lift coefficient and C_T is the torsion coefficient (Figure 3).

$$C_D = \left(\phi_x^2 + \phi_y^2\right) C_x \tag{6a}$$

$$C_L = \left(\phi_x^2 + \phi_y^2\right) C_y \tag{6b}$$

$$C_T = b\left(\phi_x^2 + \phi_y^2\right) C_M \tag{6c}$$

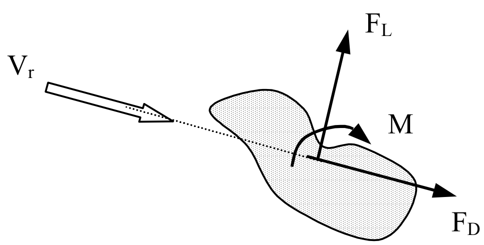

Figure 3: Aerodynamic forces

The aerodynamic forces depend on coefficients that characterize the flow at the body location (ϕ_x, ϕ_y, $\phi_{x,x}$, etc.) and other factors that depend on the cross-sectional shape of the body (C_x, $C_{x,\alpha}$, C_y, etc.). Both groups of values can be determined by independents experiments in wind tunnel and, in the same way, it is possible to combine numerical evaluations of flow functions with coefficients experimentally determined. These coefficients are shown in the matrices ***A*** and ***B***, whose components are:

$$A_{11} = 2C_x\left(\phi_x\phi_{x,x} + \phi_y\phi_{y,x}\right) - \phi_x C_{x,\alpha}\left(1+\overline{\alpha}_0^2\right)\left(\phi_{y,x} - \overline{\alpha}_0\phi_{x,x}\right) \quad (7a)$$

$$A_{12} = 2C_x\left(\phi_x\phi_{x,y} + \phi_y\phi_{y,y}\right) - \phi_x C_{x,\alpha}\left(1+\overline{\alpha}_0^2\right)\left(\phi_{y,y} - \overline{\alpha}_0\phi_{x,y}\right) \quad (7b)$$

$$A_{13} = C_{x,\alpha}(\phi_x^{\ 2} + \phi_y^{\ 2}) \quad (7c)$$

$$A_{21} = 2C_y\left(\phi_x\phi_{x,x} + \phi_y\phi_{y,x}\right) - \phi_x C_{y,\alpha}\left(1+\overline{\alpha}_0^2\right)\left(\phi_{y,x} - \overline{\alpha}_0\phi_{x,x}\right) \quad (7d)$$

$$A_{22} = 2C_y\left(\phi_x\phi_{x,y} + \phi_y\phi_{y,y}\right) - \phi_x C_{y,\alpha}\left(1+\overline{\alpha}_0^2\right)\left(\phi_{y,y} - \overline{\alpha}_0\phi_{x,y}\right) \quad (7e)$$

$$A_{23} = C_{y,\alpha}(\phi_x^{\ 2} + \phi_y^{\ 2}) \quad (7f)$$

$$A_{31} = b\left[2C_M\left(\phi_x\phi_{x,x} + \phi_y\phi_{y,x}\right) - \phi_x C_{M,\alpha}\left(1+\overline{\alpha}_0^2\right)\left(\phi_{y,x} - \overline{\alpha}_0\phi_{x,x}\right)\right] \quad (7g)$$

$$A_{32} = b\left[2C_M\left(\phi_x\phi_{x,y} + \phi_y\phi_{y,y}\right) - \phi_x C_{M,\alpha}\left(1+\overline{\alpha}_0^2\right)\left(\phi_{y,y} - \overline{\alpha}_0\phi_{x,y}\right)\right] \quad (7h)$$

$$A_{33} = bC_{M,\alpha}(\phi_x^{\ 2} + \phi_y^{\ 2}) \quad (7i)$$

$$B_{11} = \left[-2C_x\phi_x - C_{x,\alpha}\left(\phi_y + \phi_x\overline{\alpha}_0^3\right)\right]/V_0 \quad (7j)$$

$$B_{12} = \left[-2C_x\phi_y + C_{x,\alpha}\phi_x\left(1+\overline{\alpha}_0^2\right)\right]/V_0 \quad (7k)$$

$$B_{13} = C_{x,\dot{\theta}}(\phi_x^{\ 2} + \phi_y^{\ 2}) \quad (7l)$$

$$B_{21} = \left[-2C_y\phi_x - C_{y,\alpha}\left(\phi_y + \phi_x\overline{\alpha}_0^3\right)\right]/V_0 \quad (7m)$$

$$B_{22} = \left[-2C_y\phi_y + C_{y,\alpha}\phi_x\left(1+\overline{\alpha}_0^2\right)\right]/V_0 \quad (7n)$$

$$B_{23} = C_{y,\dot{\theta}}(\phi_x^{\ 2} + \phi_y^{\ 2}) \quad (7o)$$

$$B_{31} = b\left[-2C_M\phi_x - C_{M,\alpha}\left(\phi_y + \phi_x\overline{\alpha}_0^3\right)\right]/V_0 \quad (7p)$$

$$B_{32} = b\left[-2C_M\phi_y + C_{M,\alpha}\phi_x\left(1+\overline{\alpha}_0^2\right)\right]/V_0 \quad (7q)$$

$$B_{33} = bC_{M,\dot{\theta}}(\phi_x^{\ 2} + \phi_y^{\ 2}) \quad (7r)$$

4. THE STATE VARIABLES METHOD

The equations presented by Brito and Riera[1,3] must first be transformed into the frequency domain. With such purpose in mind, the following vectors are defined:

$$Q_0 = \frac{1}{2}\rho b V_0^2 \tag{8a}$$

$$\vec{p}_0 = \begin{Bmatrix} C_D \\ C_L \\ C_T \end{Bmatrix} \tag{8b}$$

Applying now the complex Fourier transform to the wind load vector, it results:

$$\vec{p} = Q_0\vec{p}_0 + Q_0\boldsymbol{A}'\begin{Bmatrix} u \\ v \\ \theta \end{Bmatrix} + (-i\omega)Q_0\boldsymbol{B}'\begin{Bmatrix} u \\ v \\ \theta \end{Bmatrix} \tag{9a}$$

$$\vec{p} = Q_0\vec{p}_0 + Q_0\boldsymbol{A}'\begin{Bmatrix} u_R + iu_I \\ v_R + iv_I \\ \theta_R + i\theta_I \end{Bmatrix} - i\omega Q_0\boldsymbol{B}'\begin{Bmatrix} u_R + iu_I \\ v_R + iv_I \\ \theta_R + i\theta_I \end{Bmatrix} \tag{9b}$$

$$\vec{p} = Q_0\vec{p}_0 + Q_0\boldsymbol{A}'\begin{Bmatrix} u_R \\ v_R \\ \theta_R \end{Bmatrix} - i\omega Q_0\boldsymbol{B}'\begin{Bmatrix} u_R \\ v_R \\ \theta_R \end{Bmatrix} + \omega Q_0\boldsymbol{B}'\begin{Bmatrix} u_I \\ v_I \\ \theta_I \end{Bmatrix} + iQ_0\boldsymbol{A}'\begin{Bmatrix} u_I \\ v_I \\ \theta_I \end{Bmatrix} \tag{9c}$$

In which ***A'*** and ***B'*** denote the transforms of matrices ***A*** and ***B*** to the frequency domain. Considering the aerodynamic forces as external loads, equations (2) become:

$$\frac{\partial \vec{v}}{\partial z} = \boldsymbol{C}\vec{v} + \vec{q}_0 \tag{10}$$

In which:

$$\boldsymbol{C} = \boldsymbol{A} + (\boldsymbol{A}' + \boldsymbol{B}'\omega)Q_0 \tag{11a}$$

$$\vec{q}_0 = \vec{q} + Q_0\vec{p}_0 \tag{11b}$$

The real and imaginary parts of vector (11b) may be shown to be:

$$\vec{q}_R(z,\omega) = \{0,\ 0,\ -q_{yR} - Q_0C_L,\ 0,\ 0,\ 0,\ -q_{xR} - Q_0C_D,\ 0,\ 0,\ 0,\ -m_{AR} - Q_0C_T,\ 0\}^T \tag{12a}$$

$$\vec{q}_I(z,\omega) = \{0,\ 0,\ -q_{yI} - Q_0C_L,\ 0,\ 0,\ 0,\ -q_{xI} - Q_0C_D,\ 0,\ 0,\ 0,\ -m_{AI} - Q_0C_T,\ 0\}^T \tag{12b}$$

$$\underbrace{(\boldsymbol{A}'+\boldsymbol{B}'\omega)Q_0}_{\vec{F}(\omega)} = \underbrace{Q_0\boldsymbol{A}'\begin{Bmatrix} u_R \\ v_R \\ \theta_R \end{Bmatrix} + \omega Q_0\boldsymbol{B}'\begin{Bmatrix} u_I \\ v_I \\ \theta_I \end{Bmatrix}}_{Real\ Part} \underbrace{- \omega Q_0\boldsymbol{B}'\begin{Bmatrix} u_R \\ v_R \\ \theta_R \end{Bmatrix} + Q_0\boldsymbol{A}'\begin{Bmatrix} u_I \\ v_I \\ \theta_I \end{Bmatrix}}_{Imaginary\ Part} \tag{12c}$$

$$\vec{F}(\omega) = \begin{Bmatrix} \vec{F}_R \\ \vec{F}_I \end{Bmatrix} = \begin{Bmatrix} Q_0\mathbf{A}'\begin{Bmatrix} u_R \\ v_R \\ \theta_R \end{Bmatrix} + Q_0\omega\mathbf{B}'\begin{Bmatrix} u_I \\ v_I \\ \theta_I \end{Bmatrix} \\ -Q_0\omega\mathbf{B}'\begin{Bmatrix} u_R \\ v_R \\ \theta_R \end{Bmatrix} + Q_0\mathbf{A}'\begin{Bmatrix} u_I \\ v_I \\ \theta_I \end{Bmatrix} \end{Bmatrix} \tag{12d}$$

In the preceding sections, the notations employed by Ambrosini *et al* [9,11] and Riera & Brito[1,3] were used for the sake of convenience and to facilitate examination of the underlying theories. At this point it must be noted, however, that:

$$u = \xi \tag{13a}$$

$$v = \eta \tag{13b}$$

Equations (12d) may then be written in the form:

$$\vec{F}(\omega) = \begin{Bmatrix} \vec{F}_R \\ \vec{F}_I \end{Bmatrix} = \begin{bmatrix} Q_0A_{22} & Q_0A_{21} & Q_0A_{23} & Q_0\omega B_{22} & Q_0\omega B_{21} & Q_0\omega B_{23} \\ Q_0A_{12} & Q_0A_{11} & Q_0A_{13} & Q_0\omega B_{12} & Q_0\omega B_{11} & Q_0\omega B_{13} \\ Q_0A_{32} & Q_0A_{31} & Q_0A_{33} & Q_0\omega B_{32} & Q_0\omega B_{31} & Q_0\omega B_{33} \\ -Q_0\omega B_{22} & -Q_0\omega B_{21} & -Q_0\omega B_{23} & Q_0A_{22} & Q_0A_{21} & Q_0A_{23} \\ -Q_0\omega B_{12} & -Q_0\omega B_{11} & -Q_0\omega B_{13} & Q_0A_{12} & Q_0A_{11} & Q_0A_{13} \\ -Q_0\omega B_{32} & -Q_0\omega B_{31} & -Q_0\omega B_{33} & Q_0A_{32} & Q_0A_{31} & Q_0A_{33} \end{bmatrix} \begin{Bmatrix} \eta_R \\ \xi_R \\ \theta_R \\ \eta_I \\ \xi_I \\ \theta_I \end{Bmatrix} \tag{14}$$

The system matrix matrix **A**, resulting from the introduction of the aerodynamic forces (14) in equation (2), is presented in Appendix A.

5. EXAMPLES

By way of illustration, two numerical applications are presented, for which other solutions, due to Riera and Brito[2], and Denardin, Nascimento and Riera[13], respectively, are already available. In the first case, a bi-dimensional radial flow in direction of a source of intensity Q, schematically shown in Figure 4, is considered.

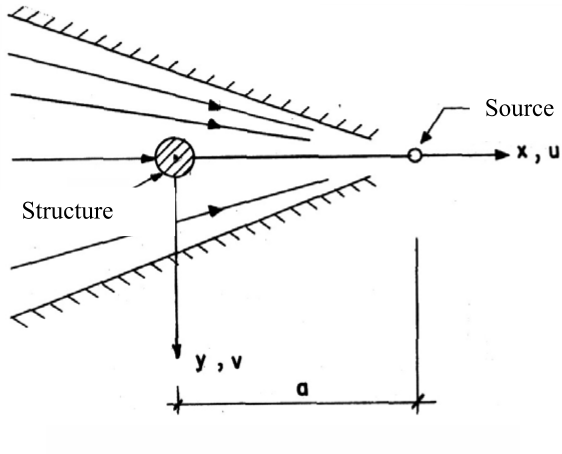

Figure 4: Structure in radial flow

The non-dimensional functions that describe this flow are well known in Hydrodynamics:

$$\phi_x = \frac{Q(a-x)}{(x-a)^2 + y^2} \tag{15a}$$

$$\phi_y = \frac{-Qy}{(x-a)^2 + y^2} \tag{15b}$$

The critical velocity determined on the basis of analytical considerations by Riera and Brito[2] for a pipe or tube parallel to the z-axis, i..e. normal to the plane of the flow defined by eqs. (15), located at x=y=0, is given by:

$$V_{0crit} = \sqrt{\frac{m\omega_x^2 a^3}{\rho b C_D Q^2}} \tag{16}$$

In the following a reinforced concrete tower 25m high with external diameter equal to 2.5m is assumed located at the origin of the coordinate system in such a flow. The mass per unit length is 400kg/m and the fundamental frequency 2.7Hz.The remaining parameters are a = 10m, Q = 100m, C_D = 0.9 and ρ = 1.226kg/m^3. The critical velocity given by equation (16) is thus 64.6m/s.

The critical velocity of the model for the complete structure described above was determined numerically by calculating its fundamental frequency for increasing values of the flow velocity. The frequency decreases as the flow velocity increases, until it becomes zero, characterizing an unstable state in which the structure is instable. The corresponding critical velocity resulted equal to 63.8m/s, differing about 1% from the analitical value indicated above.

Next, a case of aeroelastic instability induced in an aluminum straight tube will be investigated. The tube of rectangular cross-section and hinged at both ends is assumed subjected to uniform smooth wind flow parallel to the x-axis. The dimensions are indicated in Figure 5, while the structural properties are given below:

- Area of the cross-section: 1.984E-3m^2
- Moment of inertia in relation to the x axis: 1.427E-5m^4
- Moment of inertia in relation to the y axis: 2.641E-5m^4
- Aluminum specific mass: 2700kg/m^3
- Air specific mass: 1.226kg/m^3
- Young's modulus: 7.2E10N/m^2
- Fundamental frequency in x-direction: 10.72Hz
- Fundamental frequency in y-direction: 14.49Hz

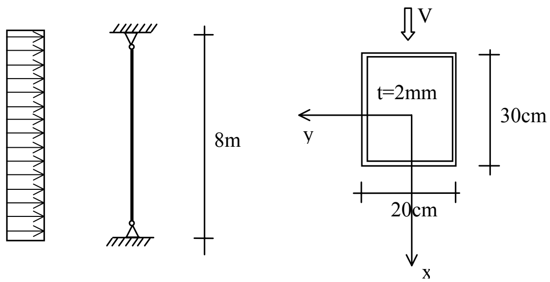

Figure 5: Tube

In this case, the nondimensional functions are $\phi_x = 1$ and $\phi_y = 0$. The critical velocity for instability in the first mode, corresponding to so-called *structural galloping*, according to Denardin, Nascimento and Riera[13] is 30.5m/s.

In case of oscillatory aerodynamic structural instability of this type, the structural damping in one or more modes of vibration decreases due to flow-structure interaction, until the total damping term becomes negative, *i.e.* the structure receives energy from the flow, becoming unstable. The procedure to determine the critical wind velocity is now as follows: the determinant of the system of equations that defines the unknown boundary conditions in the transformation of the initial value problem (2) to a two-point boundary value problem (See Ref. 12) is determined, beginning with ω= 0 for increasing values of the frequency ω until a minmum value is detected. Let ω_m denote the value of the frequency corresponding to the minimum value of the determinant. It may be shown that the natural frequency of vibration for the mode under consideration is equal to ω_m , while damping is given by $[\det(\omega_m)]^{1/2}$. Plotting this latter value in terms of the flow velocity leads to the graph in Fig. 6 which presents a minimum at a flow velocity is 30.8m/s, practically coinciding with the critical value obtained in Ref.13.

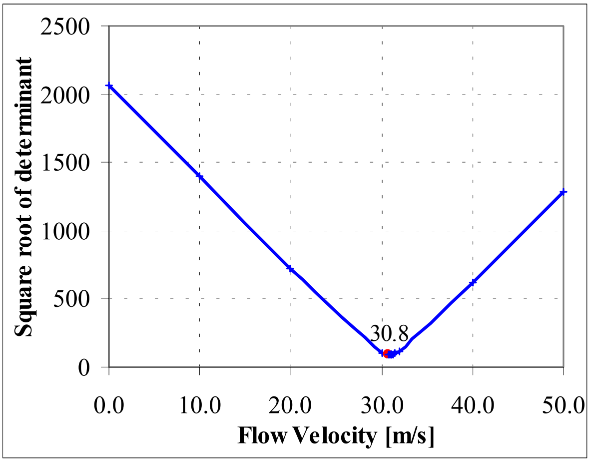

Figure 6: Determination of the critical velocity

6. CONCLUSIONS

In this paper, the field matrix in the state space formulation for the dynamic response of thin-walled, open section beams has been extended to enable the consideration of aeroelastic forces in flow-structure interaction problems. The solution is obtained in the frequency domain and presupposes linear viscoelastic behavior of the structure.

The approach is especially appropriate for assessing dynamic instability of structures subjected to wind load, from simple galloping phenomena to more complex problems involving flutter and permits as well the numerical evaluation of coupled longitudinal, transversal and torsional structural response considering the effect of fluid-structure interaction. Two simple examples are presente, illustrating the application of the method to the determination of critical flow velocities.

7. REFERENCES

[1] J. L. V. Brito and J. D. Riera, "Aerodynamic instability of cylindrical bluff bodies in non-homogeneous flow", *Journal of Wind Engineering and Industrial Aerodynamics*, **57**, 81-96 (1995).
[2] J. D. Riera and J. L. V. Brito, "Instability of pipes and cables in non-homogeneous cross-flow", *Wind and Structures*, **1**, 59-67 (1998).
[3] J. L. V. Brito and J. D. Riera, "A novel experimental approach for the determination of aerodynamic coefficients for aeroelastic instability studies", *Journal of Wind Engineering and Industrial Aerodynamics*, **84**, 289-305 (2000).
[4] D. Huston, T. Reinhold, P. Vickery and R. H. Scanlan, "Retrofitting aerodynamic perfomance of bridges. Analysis and testing", *Proc. Structures Congress 89*, San Francisco, USA, ASCE, 91-100 (1989).
[5] R. H. Scanlan and N. P. Jones, "A minimum design methodology for evaluating bridge flutter and buffeting response", *Journal of Wind Engineering and Industrial Aerodynamics*, **36**, 1341-1353 (1990).
[6] K. R. Cooper, M. Nakayama, Y. Sasaki, A. A. Fediw, S. Resende-Ide and S. J. Zan, "Unsteady aerodynamic force measurements on a super-tall building with a tapered cross section", *Journal of Wind Engineering and Industrial Aerodynamics*, **72**, 199-212 (1997).
[7] A. Larsen, "Advances in aeroelastic analyses of suspension and cable-stayed bridges", *Journal of Wind Engineering and Industrial Aerodynamics*, **74-76**, 73-90 (1998).
[8] X. Chen, M. Matsumoto and A. Kareem, "Time Domain Flutter and Buffeting Response Analyses of Bridges", *Journal of Engineering Mechanics ASCE,* **126**, 7-16 (2000).
[9] R. D. Ambrosini, J. D. Riera and R. F. Danesi, "Analysis of Structures Subjected to Random Wind Loading", *Jubileum Conference on Wind Effects on Buildings and Structures*, WEBS 98, Gramado, Brasil, Vol II, 101-108 (1998).
[10] R. D. Ambrosini, J. D. Riera and R. F. Danesi, "Dynamic Analysis of Thin-Walled and Variable Open Section Beams with Shear Flexibility", *International Journal for Numerical Methods in Engineering*, **38**, 2867-2885 (1995).
[11] R. D. Ambrosini, J. D. Riera and R. F. Danesi, "A Modified Vlasov Theory for Dynamic Analysis of Thin Walled and Variable Open Section Beams", *Engineering Structures*, **22**, 890-900 (2000).
[12] E. Pestel and F. Leckie, *Matrix Methods in Elastomechanics*, McGraw-Hill, NY, (1963).
[13] M. L. Denardin, J. A. Nascimento and J. D. Riera, "Determinação da Velocidade Crítica por Galope de Estruturas com Amortecimento Arbitrário", *Anais do IV Congresso Brasileiro de Engenharia Mecânica*, Paper A-25, 299-310 (1977).

APPENDIX A

Matrix A of equation (2)

$$
\left[\begin{array}{cccc|cccc|cccc|cccc|cccc|cccc}
0 & 1 & \frac{1}{k_y{}'FG\mu_1} & 0 & 0 & 0 & 0 & 0 & 0 & 0 & 0 & 0 & 0 & 0 & \frac{\mu}{k_y{}'FG\mu_1} & 0 & 0 & 0 & 0 & 0 & 0 & 0 & 0 & 0 \\
0 & 0 & 0 & -\frac{1}{EJ_x\mu_1} & 0 & 0 & 0 & 0 & 0 & 0 & 0 & 0 & 0 & 0 & 0 & -\frac{\mu}{EJ_x\mu_1} & 0 & 0 & 0 & 0 & 0 & 0 & 0 & 0 \\
-\rho F\omega^2 & 0 & 0 & 0 & 0 & 0 & 0 & 0 & \rho F\omega^2 a_x & 0 & 0 & 0 & 0 & 0 & 0 & 0 & 0 & 0 & 0 & 0 & 0 & 0 & 0 & 0 \\
0 & \rho J_x\omega^2 & 1 & 0 & 0 & 0 & 0 & 0 & 0 & 0 & 0 & 0 & 0 & 0 & 0 & 0 & 0 & 0 & 0 & 0 & 0 & 0 & 0 & 0 \\
\hline
0 & 0 & 0 & 0 & 0 & 1 & \frac{1}{k_x{}'FG\mu_1} & 0 & 0 & 0 & 0 & 0 & 0 & 0 & 0 & 0 & 0 & 0 & \frac{\mu}{k_x{}'FG\mu_1} & 0 & 0 & 0 & 0 & 0 \\
0 & 0 & 0 & 0 & 0 & 0 & 0 & \frac{1}{EJ_y\mu_1} & 0 & 0 & 0 & 0 & 0 & 0 & 0 & 0 & 0 & 0 & 0 & \frac{\mu}{EJ_y\mu_1} & 0 & 0 & 0 & 0 \\
0 & 0 & 0 & 0 & -\rho F\omega^2 & 0 & 0 & 0 & -\rho F\omega^2 a_y & 0 & 0 & 0 & 0 & 0 & 0 & 0 & 0 & 0 & 0 & 0 & 0 & 0 & 0 & 0 \\
0 & 0 & 0 & 0 & 0 & -\rho J_y\omega^2 & -1 & 0 & 0 & 0 & 0 & 0 & 0 & 0 & 0 & 0 & 0 & 0 & 0 & 0 & 0 & 0 & 0 & 0 \\
\hline
0 & 0 & 0 & 0 & 0 & 0 & 0 & 0 & 0 & 1 & 0 & 0 & 0 & 0 & 0 & 0 & 0 & 0 & 0 & 0 & 0 & 0 & 0 & 0 \\
0 & 0 & 0 & 0 & 0 & 0 & 0 & 0 & 0 & 0 & 0 & -\frac{1}{EJ_\varphi\mu_1} & 0 & 0 & 0 & 0 & 0 & 0 & 0 & 0 & 0 & 0 & 0 & -\frac{\mu}{EJ_\varphi\mu_1} \\
\rho F\omega^2 a_x & 0 & 0 & 0 & -\rho F\omega^2 a_y & 0 & 0 & 0 & -\rho F\omega^2 r^2 & 0 & 0 & 0 & 0 & 0 & 0 & 0 & 0 & 0 & 0 & 0 & 0 & 0 & 0 & 0 \\
0 & 0 & 0 & 0 & 0 & 0 & 0 & 0 & 0 & B\theta' & 1 & 0 & 0 & 0 & 0 & 0 & 0 & 0 & 0 & 0 & 0 & \mu GJ_d & 0 & 0 \\
\hline
0 & 0 & -\frac{\mu}{k_y{}'FG\mu_1} & 0 & 0 & 0 & 0 & 0 & 0 & 0 & 0 & 0 & 0 & 1 & \frac{1}{k_y{}'FG\mu_1} & 0 & 0 & 0 & 0 & 0 & 0 & 0 & 0 & 0 \\
0 & 0 & 0 & \frac{\mu}{EJ_x\mu_1} & 0 & 0 & 0 & 0 & 0 & 0 & 0 & 0 & 0 & 0 & 0 & -\frac{1}{EJ_x\mu_1} & 0 & 0 & 0 & 0 & 0 & 0 & 0 & 0 \\
0 & 0 & 0 & 0 & 0 & 0 & 0 & 0 & 0 & 0 & 0 & 0 & -\rho F\omega^2 & 0 & 0 & 0 & 0 & 0 & 0 & 0 & \rho F\omega^2 a_x & 0 & 0 & 0 \\
0 & 0 & 0 & 0 & 0 & 0 & 0 & 0 & 0 & 0 & 0 & 0 & 0 & \rho J_x\omega^2 & 1 & 0 & 0 & 0 & 0 & 0 & 0 & 0 & 0 & 0 \\
\hline
0 & 0 & 0 & 0 & 0 & 0 & -\frac{\mu}{k_x{}'FG\mu_1} & 0 & 0 & 0 & 0 & 0 & 0 & 0 & 0 & 0 & 0 & 1 & \frac{1}{k_x{}'FG\mu_1} & 0 & 0 & 0 & 0 & 0 \\
0 & 0 & 0 & 0 & 0 & 0 & 0 & -\frac{\mu}{EJ_y\mu_1} & 0 & 0 & 0 & 0 & 0 & 0 & 0 & 0 & 0 & 0 & 0 & \frac{1}{EJ_y\mu_1} & 0 & 0 & 0 & 0 \\
0 & 0 & 0 & 0 & 0 & 0 & 0 & 0 & 0 & 0 & 0 & 0 & 0 & 0 & 0 & 0 & -\rho F\omega^2 & 0 & 0 & 0 & -\rho F\omega^2 a_y & 0 & 0 & 0 \\
0 & 0 & 0 & 0 & 0 & 0 & 0 & 0 & 0 & 0 & 0 & 0 & 0 & 0 & 0 & 0 & 0 & -\rho J_y\omega^2 & -1 & 0 & 0 & 0 & 0 & 0 \\
\hline
0 & 0 & 0 & 0 & 0 & 0 & 0 & 0 & 0 & 0 & 0 & 0 & 0 & 0 & 0 & 0 & 0 & 0 & 0 & 0 & 0 & 1 & 0 & 0 \\
0 & 0 & 0 & 0 & 0 & 0 & 0 & 0 & 0 & 0 & 0 & \frac{\mu}{EJ_\varphi\mu_1} & 0 & 0 & 0 & 0 & 0 & 0 & 0 & 0 & 0 & 0 & 0 & -\frac{1}{EJ_\varphi\mu_1} \\
0 & 0 & 0 & 0 & 0 & 0 & 0 & 0 & 0 & 0 & 0 & 0 & \rho F\omega^2 a_x & 0 & 0 & 0 & -\rho F\omega^2 a_y & 0 & 0 & 0 & -\rho F\omega^2 r^2 & 0 & 0 & 0 \\
0 & 0 & 0 & 0 & 0 & 0 & 0 & 0 & 0 & -\mu GJ_d & 0 & 0 & 0 & 0 & 0 & 0 & 0 & 0 & 0 & 0 & 0 & B\theta' & 1 & 0
\end{array}\right]
$$

Final Matrix A including linearized flow-structures interaction effects

0	1	$\frac{1}{k_y'FG\mu_1}$	0	0	0	0	0	0	0	0	0	0	0	$\frac{\mu}{k_y'FG\mu_1}$	0	0	0	0	0	0	0	0	0
0	0	0	$-\frac{1}{EJ_x\mu_1}$	0	0	0	0	0	0	0	0	0	0	0	$-\frac{\mu}{EJ_x\mu_1}$	0	0	0	0	0	0	0	0
$-\rho F\omega^2 - Q_0A_{22}$	0	0	0	$-Q_0A_{21}$	0	0	0	$\rho F\omega^2 a_x - Q_0A_{23}$	0	0	0	$-Q_0\omega B_{22}$	0	0	0	$-Q_0\omega B_{21}$	0	0	0	$-Q_0\omega B_{23}$	0	0	0
0	$\rho J_x\omega^2$	1	0	0	0	0	0	0	0	0	0	0	0	0	0	0	0	0	0	0	0	0	0
0	0	0	0	0	1	$\frac{1}{k_x'FG\mu_1}$	0	0	0	0	0	0	0	0	0	0	0	$\frac{\mu}{k_x'FG\mu_1}$	0	0	0	0	0
0	0	0	0	0	0	0	$\frac{1}{EJ_y\mu_1}$	0	0	0	0	0	0	0	0	0	0	0	$\frac{\mu}{EJ_y\mu_1}$	0	0	0	0
$-Q_0A_{12}$	0	0	0	$-\rho F\omega^2 - Q_0A_{11}$	0	0	0	$-\rho F\omega^2 a_y - Q_0A_{13}$	0	0	0	$-Q_0\omega B_{12}$	0	0	0	$-Q_0\omega B_{11}$	0	0	0	$-Q_0\omega B_{13}$	0	0	0
0	0	0	0	0	$-\rho J_y\omega^2$	-1	0	0	0	0	0	0	0	0	0	0	0	0	0	0	0	0	0
0	0	0	0	0	0	0	0	0	1	0	0	0	0	0	0	0	0	0	0	0	0	0	0
0	0	0	0	0	0	0	0	0	0	0	$-\frac{1}{EJ_\varphi\mu_1}$	0	0	0	0	0	0	0	0	0	0	0	$-\frac{\mu}{EJ_\varphi\mu_1}$
$\rho F\omega^2 a_x - Q_0A_{32}$	0	0	0	$-\rho F\omega^2 a_y - Q_0A_{31}$	0	0	0	$-\rho F\omega^2 r^2 - Q_0A_{33}$	0	0	0	$-Q_0\omega B_{32}$	0	0	0	$-Q_0\omega B_{31}$	0	0	0	$-Q_0\omega B_{33}$	0	0	0
0	0	0	0	0	0	0	0	0	$B\theta'$	1	0	0	0	0	0	0	0	0	0	0	μGJ_d	0	0
0	0	$-\frac{\mu}{k_y'FG\mu_1}$	0	0	0	0	0	0	0	0	0	0	1	$\frac{1}{k_y'FG\mu_1}$	0	0	0	0	0	0	0	0	0
0	0	0	$\frac{\mu}{EJ_x\mu_1}$	0	0	0	0	0	0	0	0	0	0	0	$-\frac{1}{EJ_x\mu_1}$	0	0	0	0	0	0	0	0
$Q_0\omega B_{22}$	0	0	0	$Q_0\omega B_{21}$	0	0	0	$Q_0\omega B_{23}$	0	0	0	$-\rho F\omega^2 - Q_0A_{22}$	0	0	0	$-Q_0A_{21}$	0	0	0	$\rho F\omega^2 a_x - Q_0A_{23}$	0	0	0
0	0	0	0	0	0	0	0	0	0	0	0	0	$\rho J_x\omega^2$	1	0	0	0	0	0	0	0	0	0
0	0	0	0	0	0	$-\frac{\mu}{k_x'FG\mu_1}$	0	0	0	0	0	0	0	0	0	0	1	$\frac{1}{k_x'FG\mu_1}$	0	0	0	0	0
0	0	0	0	0	0	0	$-\frac{\mu}{EJ_y\mu_1}$	0	0	0	0	0	0	0	0	0	0	0	$\frac{1}{EJ_y\mu_1}$	0	0	0	0
$Q_0\omega B_{12}$	0	0	0	$Q_0\omega B_{11}$	0	0	0	$Q_0\omega B_{13}$	0	0	0	$-Q_0A_{12}$	0	0	0	$-\rho F\omega^2 - Q_0A_{11}$	0	0	0	$-\rho F\omega^2 a_y - Q_0A_{13}$	0	0	0
0	0	0	0	0	0	0	0	0	0	0	0	0	0	0	0	0	$-\rho J_y\omega^2$	-1	0	0	0	0	0
0	0	0	0	0	0	0	0	0	0	0	0	0	0	0	0	0	0	0	0	0	1	0	0
0	0	0	0	0	0	0	0	0	0	0	$\frac{\mu}{EJ_\varphi\mu_1}$	0	0	0	0	0	0	0	0	0	0	0	$-\frac{1}{EJ_\varphi\mu_1}$
$Q_0\omega B_{32}$	0	0	0	$Q_0\omega B_{31}$	0	0	0	$Q_0\omega B_{33}$	0	0	0	$\rho F\omega^2 a_x - Q_0A_{32}$	0	0	0	$-\rho F\omega^2 a_y - Q_0A_{31}$	0	0	0	$-\rho F\omega^2 r^2 - Q_0A_{33}$	0	0	0
0	0	0	0	0	0	0	0	0	$-\mu GJ_d$	0	0	0	0	0	0	0	0	0	0	0	$B\theta'$	1	0